Chapter-5

Influence of magnetic field on Hyperbolic tangent fluid through a porous medium in a planar channel with Peristalsis

5.1 Introduction

Peristaltic transport is a form of fluid transport generated by a progressive wave of area contraction or expansion along a length of a distensible tube containing fluid. Peristaltic transport widely occurs in many biological systems for example, food swallowing through the esophagus, intra-urine fluid motion, circulation of blood in small blood vessels and the flows of many other glandular ducts. Several theoretical and experimental studies have been undertaken to understand peristalsis through abrupt changes in geometry and realistic assumptions. Peristaltic transport of Newtonian fluids has been studied by Fung and Yih (1968)[23], Shapiro et al. (1969)[50] and Subba Reddy et al. (2005)[[62] under different conditions.

It is well known that most physiological fluids including blood behave as non-Newtonian fluids. Hence, the study of peristaltic transport of non-Newtonian fluids may help to get better understanding of the working biological systems. One especial class of fluids which are of considerable practical importance is that in which the viscosity depends on the shear stress or on the flow rate. The viscosity of most non-Newtonian fluids, such as polymers, is usually a nonlinear decreasing function of the generalized shear rate. This is known as shear-thinning behavior. Such fluid is a hyperbolic tangent fluid (Ai and Vafai, 2005[4]). The peristaltic transport of a hyperbolic tangent fluid in an asymmetric channel was discussed by Nadeem and Akram (2009)[[42]. Nadeem and Akram (2011)[44] have studied the effect of magnetic field on the peristaltic motion of a hyperbolic tangent fluid in a vertical asymmetric channel with heat transfer. The peristaltic transport of a Tangent hyperbolic fluid in an endoscope numerically was investigated by Nadeem and Akbar (2011)[45]. Akbar et al. (2012)[6] have studied the effects of slip and heat transfer on the peristaltic transport of a hyperbolic tangent fluid in an inclined asymmetric channel.

The study of MHD flows is quite attractive and useful because it is used in magnetic wound or cancer tumor treatment causing hypothermia, bleeding reduction during surgeries, targeted transport of drugs using magnetic particles as drug carries and MRI (magnetic resonance imaging) to diagnose the disease. Some significant studies involving MHD flows were discussed by Srivastava and Agrawal (1980)[57] and Agrwal and Anwaruddin (1984)[3]. The effects of the magnetic field on the peristalsis are also significant in connection with certain problems of the movement of the conductive physiological fluids, e.g., the blood and blood pump machines. Peristaltic transport of a MHD third order fluid in a circular cylindrical tube was investigated by Hayat and Ali (2006)[28]. Hayat et al. (2007)[[29] studied peristaltic transport of a third order fluid in a uniform channel under the effect of a magnetic field. Hayat et al. (2007)[30] developed the peristaltic flow of a fourth grade fluid under the effect of a magnetic field in a planar channel. Subba Reddy and Gangadhar (2010)[64] have studied the peristaltic motion of a Carreau fluid under the effect of a magnetic field in an inclined planar channel. Subba Reddy et al. (2011)[66] have investigated the peristaltic pumping of Williamson fluid in a planar channel under the effect of magnetic field.

A porous medium is the matter which contains a number of small holes distributed throughout the matter. Flows through a porous medium occur in filtration of fluids. Hall effects on peristaltic flow of a Maxwell fluid in a porous medium were investigated by Hayat et al. (2007)[31]. El-Dabe et al. (2010)[15] have discussed the effect of magnetic field on the peristaltic motion of a Carreau fluid through a porous medium with heat transfer. Peristaltic motion of a couple stress fluid through a porous medium in a channel with slip condition was studied by Alemayehu and Radhakrishnamacharya (2010)[47]. Suryanarayana Reddy et al. (2011)[70] have studied the peristaltic MHD flow of a Bingham fluid through a porous medium in a channel.

In view of these, we studied the effect of MHD on the peristaltic transport of a hyperbolic tangent fluid through a porous medium in a planar channel under the assumptions of low Reynolds number and long wavelength. The expression for the velocity and axial pressure gradient are obtained by employing perturbation technique. The effects of various pertinent parameters on the axial pressure gradient and time-averaged flow rate are discussed with the aid of graphs.

This chapter was published in **International journal of Mathematical Archive, 4(8), 2013, 171-182.**

5.2 Mathematical Formulation

We consider the peristaltic motion of a hyperbolic tangent fluid through a porous medium in a two-dimensional symmetric channel of width $2a$. The flow is generated by sinusoidal wave trains propagating with constant speed c along the channel walls. The fluid subjected to a constant transverse magnetic field. Induced magnetic field, external electric field, electric field due to polarization of charges, heat due to viscous and joule dissipation are neglected. Fig. 5.1 shows the schematic diagram of the channel.

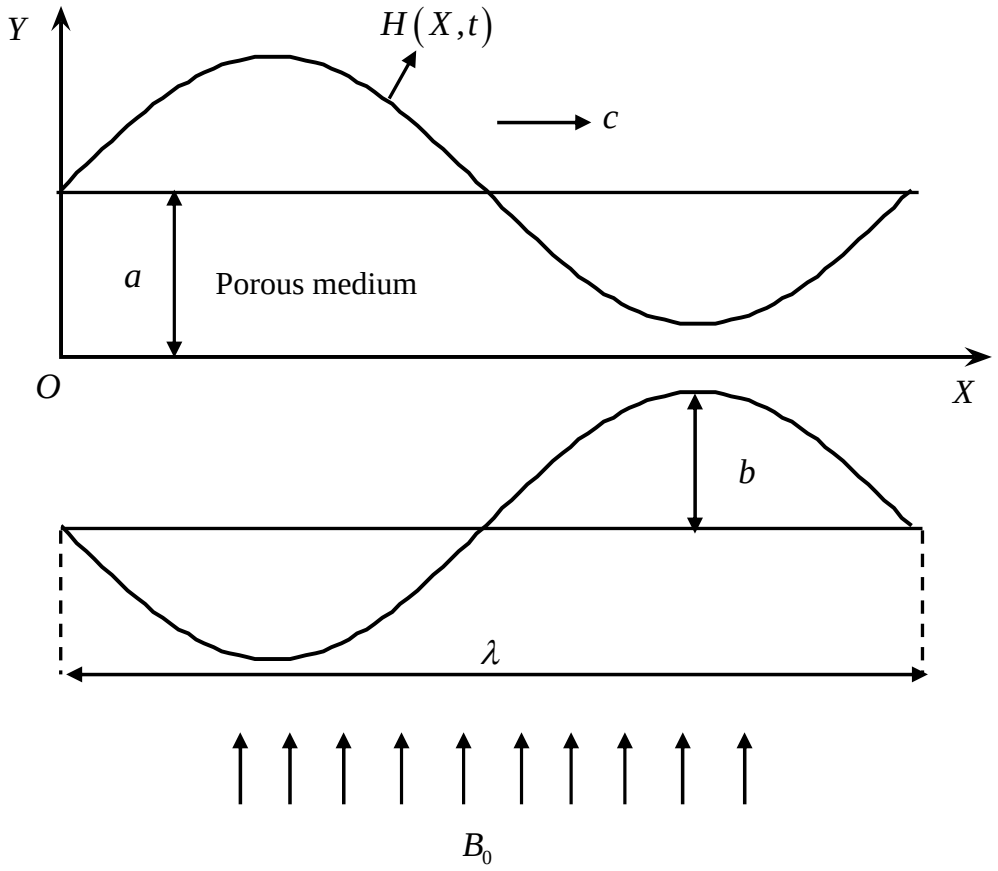

Fig. 5.1 The physical model

The wall deformation is given by

$$Y = \pm H(X,t) = \pm a \pm b\sin\frac{2\pi}{\lambda}(X - ct) \qquad (5.2.1)$$

where *b* is the amplitude of the wave, λ - the wave length and X and Y - the rectangular co-ordinates with X measured along the axis of the channel and Y perpendicular to X. Let (U,V) be the velocity components in fixed frame of reference (X,Y).

The flow is unsteady in the laboratory frame (X,Y). However, in a co-ordinate system moving with the propagation velocity c (wave frame (*x, y*)), the boundary shape is stationary. The transformation from fixed frame to wave frame is given by

$$x = X - ct, y = Y, u = U - c, v = V \tag{5.2.2}$$

where (u,v) and (U,V) are velocity components in the wave and laboratory frames respectively.

The constitutive equation for a Hyperbolic Tangent fluid is

$$\tau = -\left[\eta_\infty + \left(\eta_0 + \eta_\infty\right)\tanh\left(\Gamma\dot{\gamma}\right)^n\right]\dot{\gamma} \tag{5.2.3}$$

where τ is the extra stress tensor, η_∞ is the infinite shear rate viscosity, η_o is the zero shear rate viscosity, Γ is the time constant, n is the power-law index and $\dot{\gamma}$ is defined as

$$\dot{\gamma} = \sqrt{\frac{1}{2}\sum_i\sum_j \dot{\gamma}_{ij}\dot{\gamma}_{ji}} = \sqrt{\frac{1}{2}\pi} \tag{5.2.4}$$

where π is the second invariant stress tensor. We consider in the constitutive equation (5.2.3) the case for which $\eta_\infty = 0$ and $\Gamma\dot{\gamma} < 1$, so the Eq. (5.2.3) can be written as

$$\tau = -\eta_0\left(\Gamma\dot{\gamma}\right)^n\dot{\gamma} = -\eta_0\left(1+\Gamma\dot{\gamma}-1\right)^n\dot{\gamma} = -\eta_0\left(1+n\left[\Gamma\dot{\gamma}-1\right]\right)\dot{\gamma} \tag{5.2.5}$$

The above model reduces to Newtonian for $\Gamma = 0$ and $n = 0$.

The equations governing the flow in the wave frame of reference are

$$\frac{\partial u}{\partial x} + \frac{\partial v}{\partial y} = 0 \tag{5.2.6}$$

$$\rho\left(u\frac{\partial u}{\partial x} + v\frac{\partial u}{\partial y}\right) = -\frac{\partial p}{\partial x} - \frac{\partial \tau_{xx}}{\partial x} - \frac{\partial \tau_{yx}}{\partial y} - \left(\sigma B_0^2 + \frac{\eta_0}{k}\right)\left(u + c\right) \tag{5.2.7}$$

$$\rho\left(u\frac{\partial v}{\partial x} + v\frac{\partial u}{\partial y}\right) = -\frac{\partial p}{\partial y} - \frac{\partial \tau_{xy}}{\partial x} - \frac{\partial \tau_{yy}}{\partial y} - \frac{\eta_0}{k}v \tag{5.2.8}$$

where ρ is the density σ is the electrical conductivity, B_0 is constant transverse magnetic field and k is the permeability of the porous medium.

The corresponding dimensional boundary conditions are

$$u = -c \qquad \text{at} \qquad y = H \tag{5.2.9}$$

$$\frac{\partial u}{\partial y} = 0 \qquad \text{at} \qquad y = 0 \tag{5.2.10}$$

Introducing the non-dimensional variables defined by

$$\bar{x} = \frac{x}{\lambda},\ \bar{y} = \frac{y}{a},\ \bar{u} = \frac{u}{c},\ \bar{v} = \frac{v}{c\delta},\ \delta = \frac{a}{\lambda},\ \bar{p} = \frac{pa^2}{\eta_0 c\lambda}, \phi = \frac{b}{a}$$

$$h = \frac{H}{a},\ \bar{t} = \frac{ct}{\lambda},\ \bar{\tau}_{xx} = \frac{\lambda}{\eta_0 c}\tau_{xx},\ \bar{\tau}_{xy} = \frac{a}{\eta_0 c}\tau_{xy},\ \bar{\tau}_{yy} = \frac{\lambda}{\eta_0 c}\tau_{yy},$$

$$\mathrm{Re} = \frac{\rho ac}{\eta_0},\ We = \frac{\Gamma c}{a},\ \bar{\dot{\gamma}} = \frac{\dot{\gamma} a}{c},\ \bar{q} = \frac{q}{ac} \tag{5.2.11}$$

into the Equations (5.2.6) - (5.2.8), reduce to (after dropping the bars)

$$\frac{\partial u}{\partial x} + \frac{\partial v}{\partial y} = 0 \tag{5.2.12}$$

$$\mathrm{Re}\,\delta\left(u\frac{\partial u}{\partial x} + v\frac{\partial u}{\partial y}\right) = -\frac{\partial p}{\partial x} - \delta^2\frac{\partial \tau_{xx}}{\partial x} - \frac{\partial \tau_{xy}}{\partial y} - \left(M^2 + \frac{1}{Da}\right)(u+1) \tag{5.2.13}$$

$$\mathrm{Re}\,\delta^3\left(u\frac{\partial v}{\partial x} + v\frac{\partial v}{\partial y}\right) = -\frac{\partial p}{\partial y} - \delta^2\frac{\partial \tau_{xy}}{\partial y} - \delta\frac{\partial \tau_{yy}}{\partial y} - \frac{\delta^2}{Da}v \tag{5.2.14}$$

where $\tau_{xx} = -2\left[1 + n\left(We\dot{\gamma} - 1\right)\right]\frac{\partial u}{\partial x}$, $\qquad \tau_{xy} = -\left[1 + n\left(We\dot{\gamma} - 1\right)\right]\left(\frac{\partial u}{\partial y} + \delta^2\frac{\partial v}{\partial x}\right)$,

$$\tau_{yy} = -2\delta\left[1 + n\left(We\dot{\gamma} - 1\right)\right]\frac{\partial v}{\partial y},\ \dot{\gamma} = \left[2\delta^2\left(\frac{\partial u}{\partial x}\right)^2 + \left(\frac{\partial u}{\partial y} + \delta^2\frac{\partial v}{\partial x}\right)^2 + 2\delta^2\left(\frac{\partial v}{\partial y}\right)^2\right]^{\frac{1}{2}}$$

$M = aB_0\sqrt{\frac{\sigma}{\eta_0}}$ is the Hartmann number and $Da = \frac{k}{a^2}$ is the Darcy number.

Under lubrication approach, neglecting the terms of order δ and Re, the Equations (5.2.13) and (5.2.14) become

$$\frac{\partial p}{\partial x}=\frac{\partial}{\partial y}\left\{\left[1+n\left(We\frac{\partial u}{\partial y}-1\right)\right]\frac{\partial u}{\partial y}\right\}-\left(M^2+\frac{1}{Da}\right)(u+1) \tag{5.2.15}$$

$$\frac{\partial p}{\partial y}=0 \tag{5.2.16}$$

From Eq. (5.2.15) and (5.2.16), we get

$$\frac{dp}{dx}=(1-n)\frac{\partial^2 u}{\partial y^2}+nWe\frac{\partial}{\partial y}\left[\left(\frac{\partial u}{\partial y}\right)^2\right]-\alpha^2(u+1) \tag{5.2.17}$$

where $\alpha=\sqrt{M^2+\frac{1}{Da}}$.

The corresponding non-dimensional slip boundary conditions in the wave frame are given by

$$u=-1 \qquad \text{at} \qquad y=h=1+\phi\sin 2\pi x \tag{5.2.18}$$

$$\frac{\partial u}{\partial y}=0 \qquad \text{at} \qquad y=0 \tag{5.2.19}$$

The volume flow rate q in a wave frame of reference is given by

$$q=\int_0^h u\,dy\,. \tag{5.2.20}$$

The instantaneous flow $Q(X,t)$ in the laboratory frame is

$$Q(X,t)=\int_0^h U\,dY=\int_0^h (u+1)\,dy=q+h \tag{5.2.21}$$

The time averaged volume flow rate $\overline{Q}$ over one period $T\left(=\frac{\lambda}{c}\right)$ of the peristaltic wave is given by

$$\overline{Q}=\frac{1}{T}\int_0^T Q\,dt=q+1 \tag{5.2.22}$$

5.3. Solution

Since Eq. (5.2.17) is a non-linear differential equation, it is not possible to obtain closed form solution. Therefore we employ regular perturbation to find the solution.

For perturbation solution, we expand $u, \frac{dp}{dx}$ and q as follows

$$u = u_0 + We\, u_1 + O\left(We^2\right) \tag{5.3.1}$$

$$\frac{dp}{dx} = \frac{dp_0}{dx} + We\frac{dp_1}{dx} + O\left(We^2\right) \tag{5.3.2}$$

$$q = q_0 + We\, q_1 + O\left(We^2\right) \tag{5.3.3}$$

Substituting these equations into the Eqs. (5.2.17) - (5.2.19), we obtain

5.3.1. System of order We^0

$$(1-n)\frac{\partial^2 u_0}{\partial y^2} - \alpha^2 u_0 = \frac{dp_0}{dx} + \alpha^2 \tag{5.3.4}$$

and the respective boundary conditions are

$$u_0 = -1 \qquad \text{at} \qquad y = h \tag{5.3.5}$$

$$\frac{\partial u_0}{\partial y} = 0 \qquad \text{at} \qquad y = 0 \tag{5.3.6}$$

5.3.2. System of order We^1

$$(1-n)\frac{\partial^2 u_1}{\partial y^2} - \alpha^2 u_1 = \frac{dp_1}{dx} - \frac{\partial}{\partial y}\left[\left(\frac{\partial u_o}{\partial y}\right)^2\right] \tag{5.3.7}$$

and the respective boundary conditions are

$$u_1 = 0 \qquad \text{at} \qquad y = h \tag{5.3.8}$$

$$\frac{\partial u_1}{\partial y} = 0 \qquad \text{at} \qquad y = 0 \tag{5.3.9}$$

5.3.3 Solution for system of order We^0

Solving Eq. (5.3.4) using the boundary conditions (5.3.5) and (5.3.6), we obtain

$$u_0 = \frac{1}{\alpha_1^2(1-n)}\frac{dp_0}{dx}\left[\frac{\cosh \alpha_1 y}{\cosh \alpha_1 h} - 1\right] - 1 \tag{5.3.10}$$

where $\alpha_1 = \alpha / \sqrt{(1-n)}$.

The volume flow rate q_0 is given by

$$q_0 = \frac{1}{\alpha_1^3(1-n)}\frac{dp_0}{dx}\left[\frac{\sinh\alpha_1 h - \alpha_1 h\cosh\alpha_1 h}{\cosh\alpha_1 h}\right] - h \tag{5.3.11}$$

From Eq. (5.3.11), we have

$$\frac{dp_0}{dx} = \frac{(q_0+h)\alpha_1^2(1-n)\cosh\alpha_1 h}{\left[\sinh\alpha_1 h - \alpha_1 h\cosh\alpha_1 h\right]} \tag{5.3.12}$$

5.3.4 Solution for system of order We^1

Substituting Eq. (5.3.10) in the Eq. (5.3.7) and solving the Eq. (5.3.7), using the boundary conditions (5.3.8) and (5.3.9), we obtain

$$\begin{aligned} u_1 = {} & \frac{1}{\alpha_1^2(1-n)}\frac{dp_1}{dx}\left[\frac{\cosh\alpha_1 y}{\cosh\alpha_1 h} - 1\right] \\ & + \frac{n}{3}\frac{\left(\frac{dp_0}{dx}\right)^2}{\left[\alpha_1(1-n)\cosh\alpha_1 h\right]^3}\left[\begin{array}{l}(\sinh 2\alpha_1 h - 2\sinh\alpha_1 h)\cosh\alpha_1 y \\ +(2\sinh\alpha_1 y - \sinh 2\alpha_1 y)\cosh\alpha_1 h\end{array}\right] \end{aligned} \tag{5.3.13}$$

The volume flow rate q_1 is given by

$$q_1 = \frac{1}{\alpha_1^2(1-n)}\frac{dp_1}{dx}\left[\frac{\sinh\alpha_1 h - \alpha_1 h\cosh\alpha_1 h}{\cosh\alpha_1 h}\right] + \frac{An}{6\alpha_1^2(1-n)^3}\left(\frac{dp_0}{dx}\right)^2\frac{1}{\cosh^3\alpha_1 h} \tag{5.3.14}$$

where $A = 4 - \cosh\alpha_1 h + 2\sinh 2\alpha_1 h\sinh\alpha_1 h - \cosh\alpha_1 h\cosh 2\alpha_1 h$.

From Eq. (5.3.14) and (5.3.12), we have

$$\frac{dp_1}{dx} = \frac{q_1\alpha_1^3(1-n)\cosh\alpha_1 h}{\left[\sinh\alpha_1 h - \alpha_1 h\cosh\alpha_1 h\right]} - \frac{An}{6\alpha_1(1-n)^2}\frac{\left(\frac{dp_0}{dx}\right)^2}{\cosh^2\alpha_1 h(\sinh\alpha_1 h - \alpha_1 h\cosh\alpha_1 h)} \tag{5.3.15}$$

Substituting Equations (5.3.12) and (5.3.15) into the Eq. (5.3.2) and using the relation $\frac{dp_0}{dx} = \frac{dp}{dx} - We\frac{dp_1}{dx}$ and neglecting terms greater than $O(We)$, we get

$$\frac{dp}{dx} = \frac{(q+h)\alpha_1^3(1-n)\cosh\alpha_1 h}{\left[\sinh\alpha_1 h - \alpha_1 h\cosh\alpha_1 h\right]} - \frac{WeAn\alpha_1^5}{6}\frac{(q+h)^2}{(\sinh\alpha_1 h - \alpha_1 h\cosh\alpha_1 h)^3} \tag{5.3.16}$$

The dimensionless pressure rise per one wavelength in the wave frame is defined as

$$\Delta p = \int_0^1 \frac{dp}{dx} dx \tag{5.3.17}$$

Note that, as $M \to 0$, $Da \to \infty$, $We \to 0$ and $n \to 0$ our results coincide with the results of Shapiro et al. (1969).

5.4. Results and Discussions

Fig. 5.2 shows the variation of axial pressure gradient $\frac{dp}{dx}$ with We for $\phi = 0.6$, $n = 0.5$, $M = 1$, $\overline{Q} = -1$ and $Da = 0.1$. It is observed that, the axial pressure gradient $\frac{dp}{dx}$ increases with increasing We.

The variation of axial pressure gradient $\frac{dp}{dx}$ with n for $\phi = 0.6$, $We = 0.01$, $M = 1$, $\overline{Q} = -1$ and $Da = 0.1$ is shown in Fig. 5.3. It is found that, the axial pressure gradient $\frac{dp}{dx}$ decreases with increasing n.

Fig. 5.4 depicts the variation of axial pressure gradient $\frac{dp}{dx}$ with Da for $\phi = 0.6$, $M = 1$, $n = 0.5$, $\overline{Q} = -1$ and $We = 0.01$. It is noted that, the axial pressure gradient $\frac{dp}{dx}$ decreases with increasing Da.

The variation of axial pressure gradient $\frac{dp}{dx}$ with M for $\phi = 0.6$, $Da = 0.1$, $n = 0.5$, $\overline{Q} = -1$ and $We = 0.01$ is depicted in Fig. 5.5. It is observed that, the axial pressure gradient $\frac{dp}{dx}$ increases with increasing M.

Fig. 5.6 illustrates the variation of axial pressure gradient $\frac{dp}{dx}$ with ϕ for $Da = 0.1$, $M = 1$, $n = 0.5$, $\overline{Q} = -1$ and $We = 0.01$. It is found that, the axial pressure gradient $\frac{dp}{dx}$ increases with increasing ϕ.

The variation of pressure rise Δp with time-averaged volume flow rate $\overline{Q}$ for different values of We with $\phi = 0.6, M = 1$, $n = 0.5$ and $Da = 0.1$ is illustrated in Fig. 5.7. It is noted that, the time-averaged volume flow rate $\overline{Q}$ increases with increasing We in pumping $(\Delta p > 0)$, free-pumping $(\Delta p = 0)$ and co-pumping $(\Delta p < 0)$ regions.

Fig. 5.8 shows the variation of pressure rise Δp with time-averaged volume flow rate $\overline{Q}$ for different values of n with $\phi = 0.6$, $M = 1$, $We = 0.01$ and $Da = 0.1$. It is observed that, the time-averaged volume flow rate $\overline{Q}$ decreases with an increase in n in both the pumping and free pumping regions, while it increases with increasing n in co-pumping region for chosen $\Delta p(< 0)$.

The variation of pressure rise Δp with time-averaged volume flow rate $\overline{Q}$ for different values of Da with $\phi = 0.6, M = 1$, $n = 0.5$ and $We = 0.01$ is shown in Fig. 5.9. It is noted that, the time-averaged volume flow rate $\overline{Q}$ decreases with increasing Da in the pumping region, while it increases with increasing Da in both the free-pumping and co-pumping regions.

Fig. 5.10 depicts the variation of pressure rise Δp with time-averaged volume flow rate $\overline{Q}$ for different values of M with $We = 0.01, \phi = 0.6$, $n = 0.5$ and $Da = 0.1$. It is found that, the time-averaged volume flow rate $\overline{Q}$ increases with an increase in M in the pumping region, while it decreases with increasing M in both the free-pumping and co-pumping regions.

The variation of pressure rise Δp with time-averaged volume flow rate $\overline{Q}$ for different values of ϕ with $We = 0.01, M = 1$, $n = 0.5$ and $Da = 0.1$ is depicted in

Fig. 5.11. It is found that, the time-averaged volume flow rate $\overline{Q}$ increases with an increase in ϕ in both the pumping and free-pumping regions, while it decreases with increasing ϕ in the co-pumping region for chosen $\Delta p(<0)$.

5.5 Conclusions

In this chapter, we studied the peristaltic flow of a hyperbolic tangent fluid through a porous medium in a planar channel under the assumptions of low Reynolds number and long wavelength. The expression for the velocity and axial pressure gradient are obtained by employing perturbation technique. It is observed that, the axial pressure gradient increases with increasing We, M and ϕ, while it decreases with increasing n and Da. Also, it is observed that in the pumping region the time-averaged flow rate $\overline{Q}$ increases with increasing We and ϕ, while it decreases with increasing n and Da. Further, it is observed that the pumping is less for hyperbolic tangent fluid than that of Newtonian fluid.

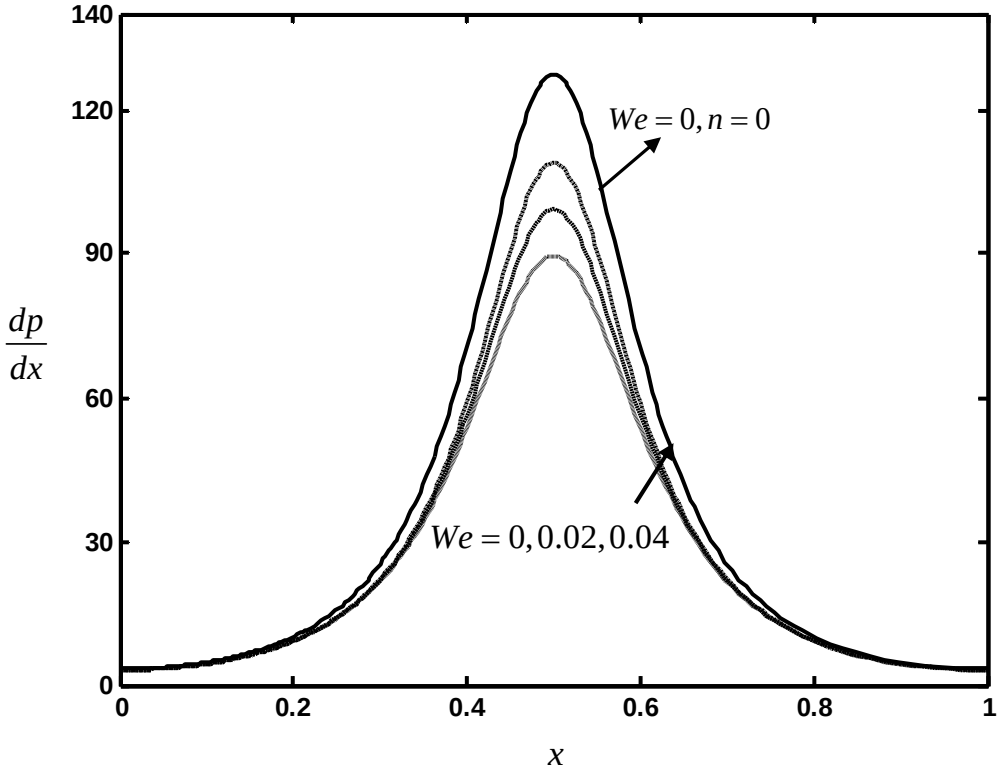

Fig. 5.2 The variation of axial pressure gradient $\frac{dp}{dx}$ with We for $\phi = 0.6$, $n = 0.5$, $M = 1$, $\overline{Q} = -1$ and $Da = 0.1$.

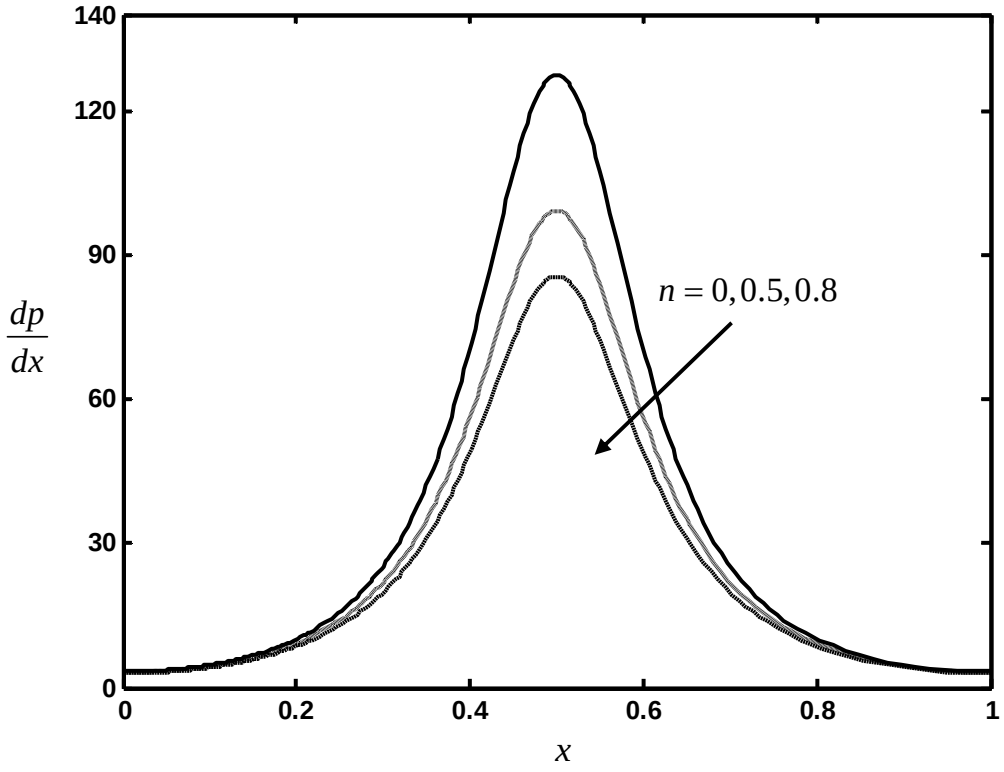

Fig. 5.3 The variation of axial pressure gradient $\frac{dp}{dx}$ with n for $\phi = 0.6$, $We = 0.01$, $M = 1$, $\overline{Q} = -1$ and $Da = 0.1$.

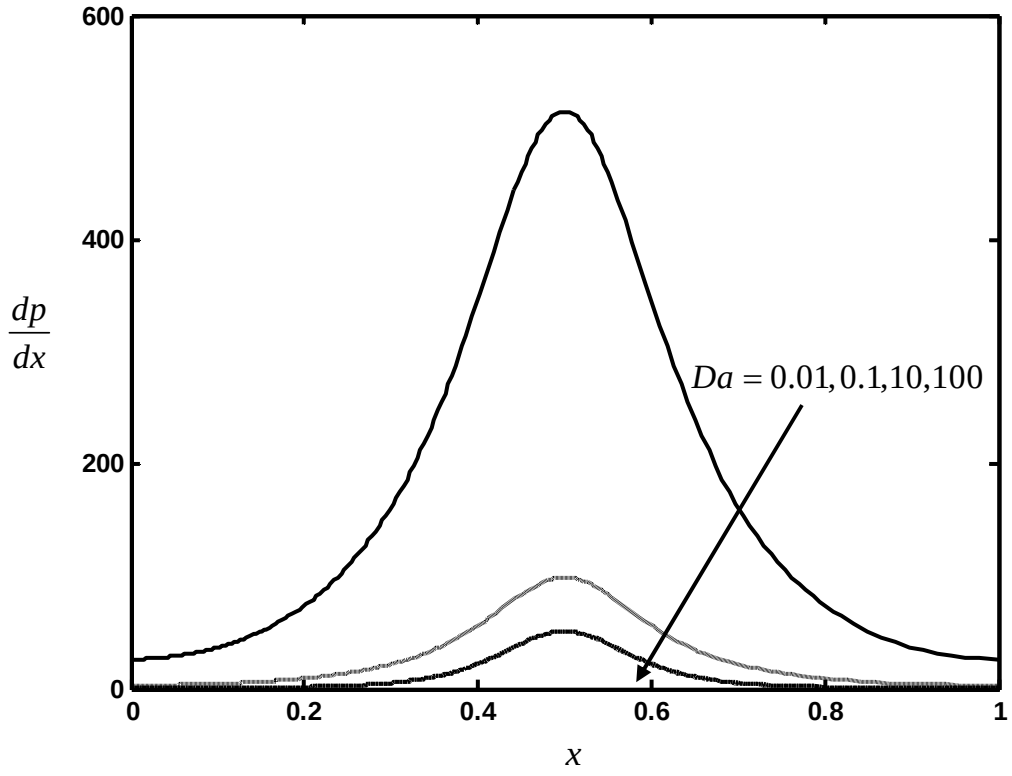

Fig. 5.4 The variation of axial pressure gradient $\frac{dp}{dx}$ with Da for $\phi = 0.6$, $n = 0.5$, $M = 1$, $\overline{Q} = -1$ and $We = 0.01$.

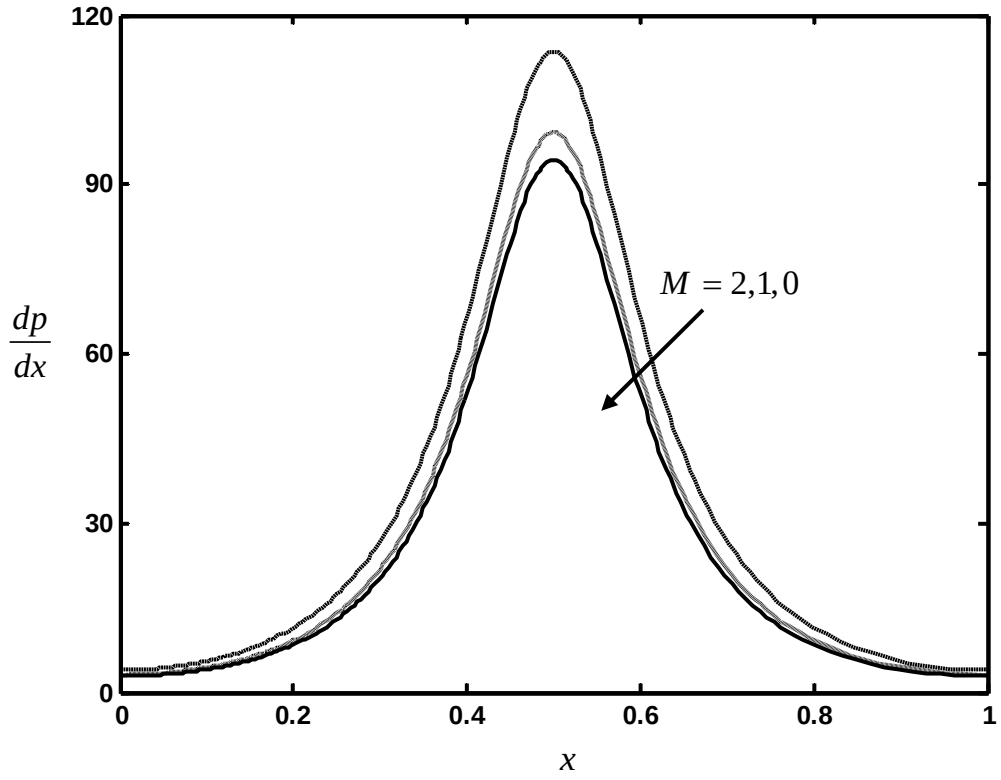

Fig. 5.5 The variation of axial pressure gradient $\frac{dp}{dx}$ with M for $\phi = 0.6$, $n = 0.5$, $Da = 0.1$, $\overline{Q} = -1$ and $We = 0.01$.

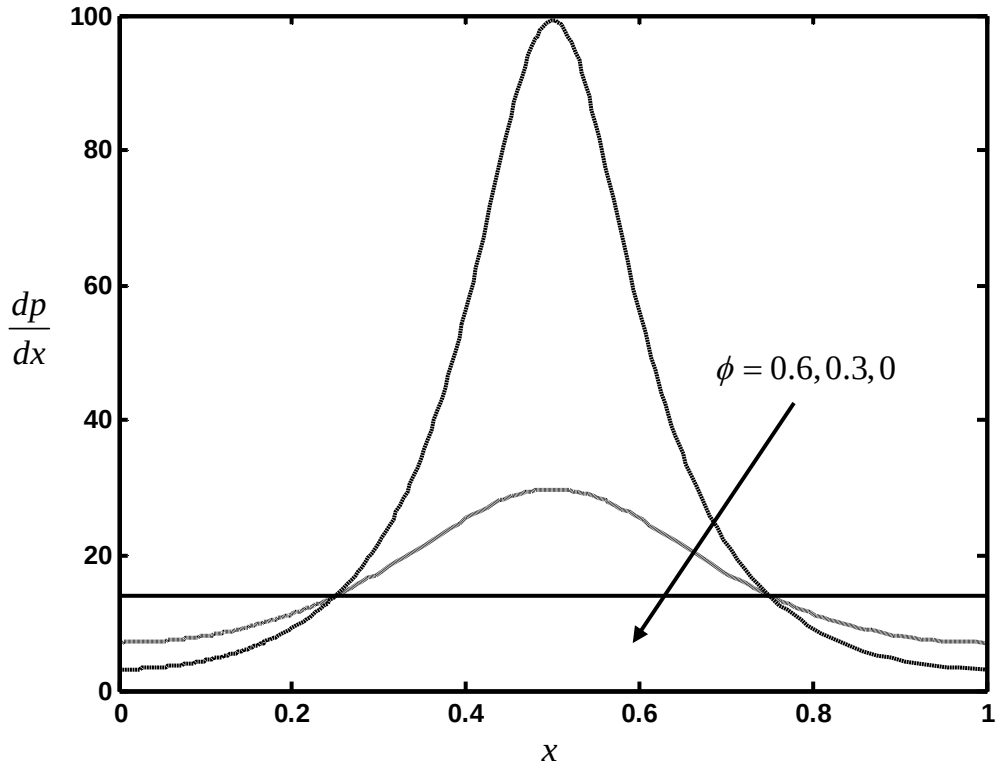

Fig. 5.6 The variation of axial pressure gradient $\frac{dp}{dx}$ with ϕ for $Da = 0.1$, $n = 0.5$, $M = 1$, $\overline{Q} = -1$ and $We = 0.01$.

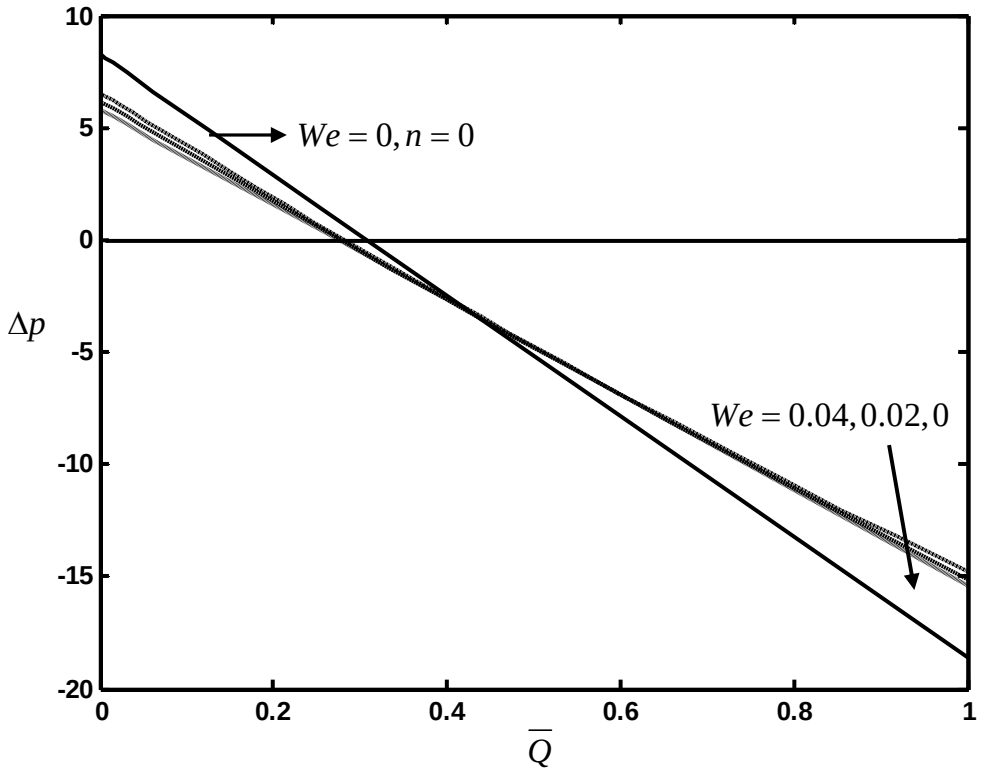

Fig. 5.7 The variation of pressure rise Δp with time-averaged volume flow rate $\overline{Q}$ for different values of We with $\phi = 0.6$, $M = 1$, $n = 0.5$ and $Da = 0.1$.

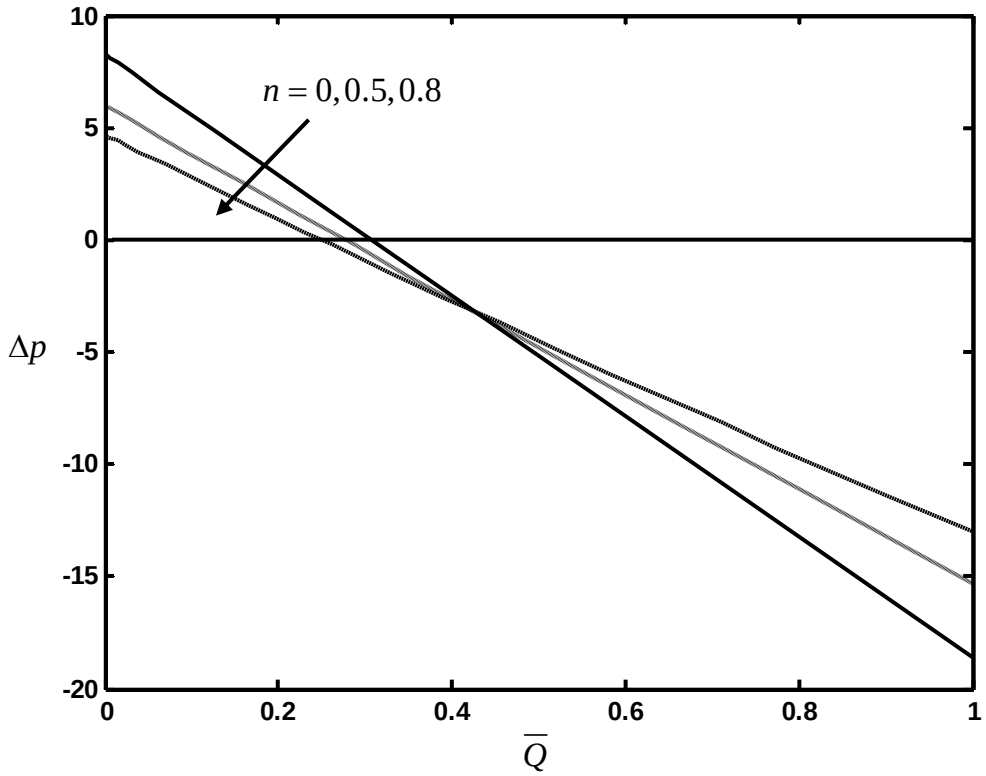

Fig. 5.8 The variation of pressure rise Δp with time-averaged volume flow rate $\overline{Q}$ for different values of n with $\phi = 0.6$, $M = 1$, $We = 0.01$ and $Da = 0.1$.

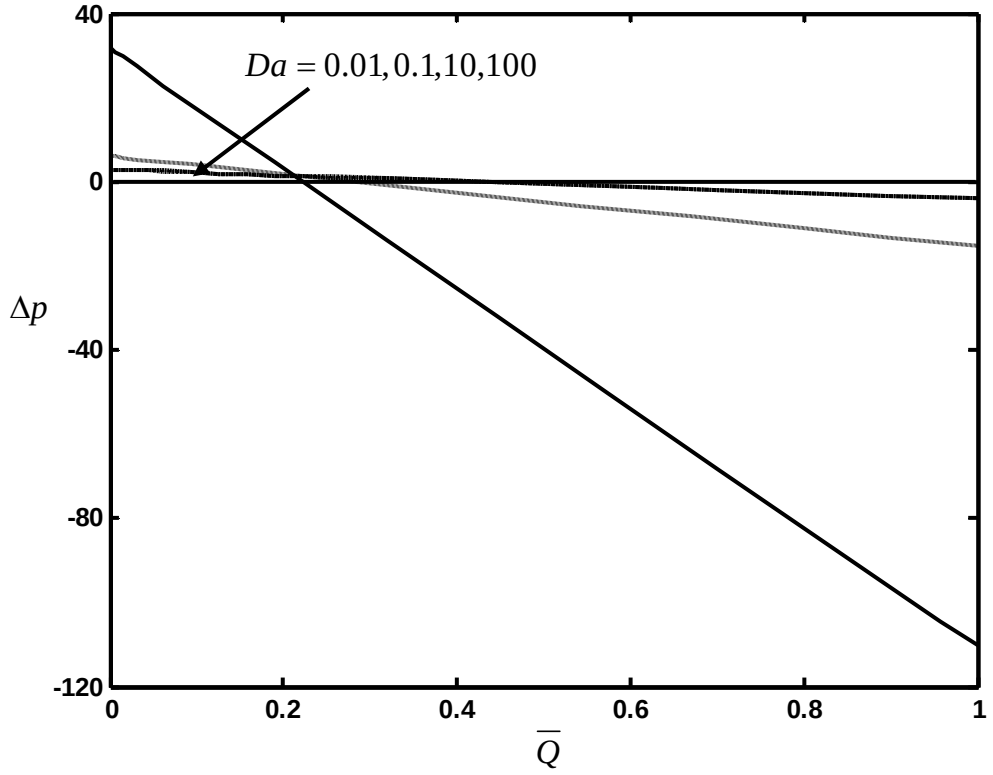

Fig. 5.9 The variation of pressure rise Δp with time-averaged volume flow rate $\overline{Q}$ for different values of Da with $\phi = 0.6, M = 1, n = 0.5$ and $We = 0.01$.

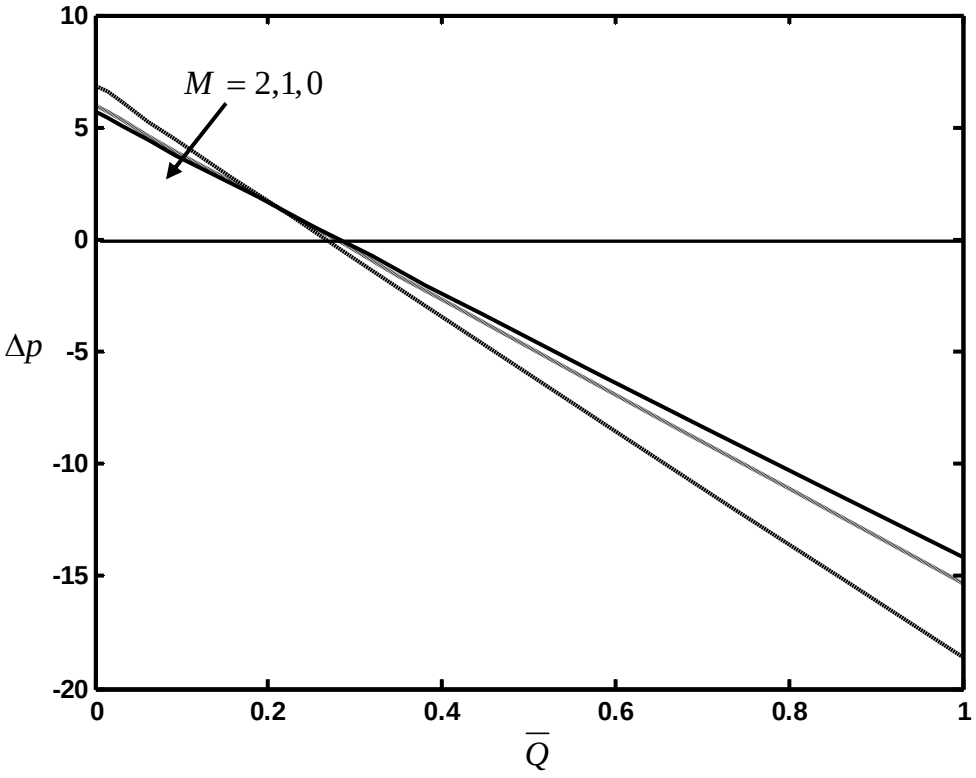

Fig. 5.10 The variation of pressure rise Δp with time-averaged volume flow rate $\overline{Q}$ for different values of M with $\phi = 0.6, Da = 0.1, n = 0.5$ and $We = 0.01$.

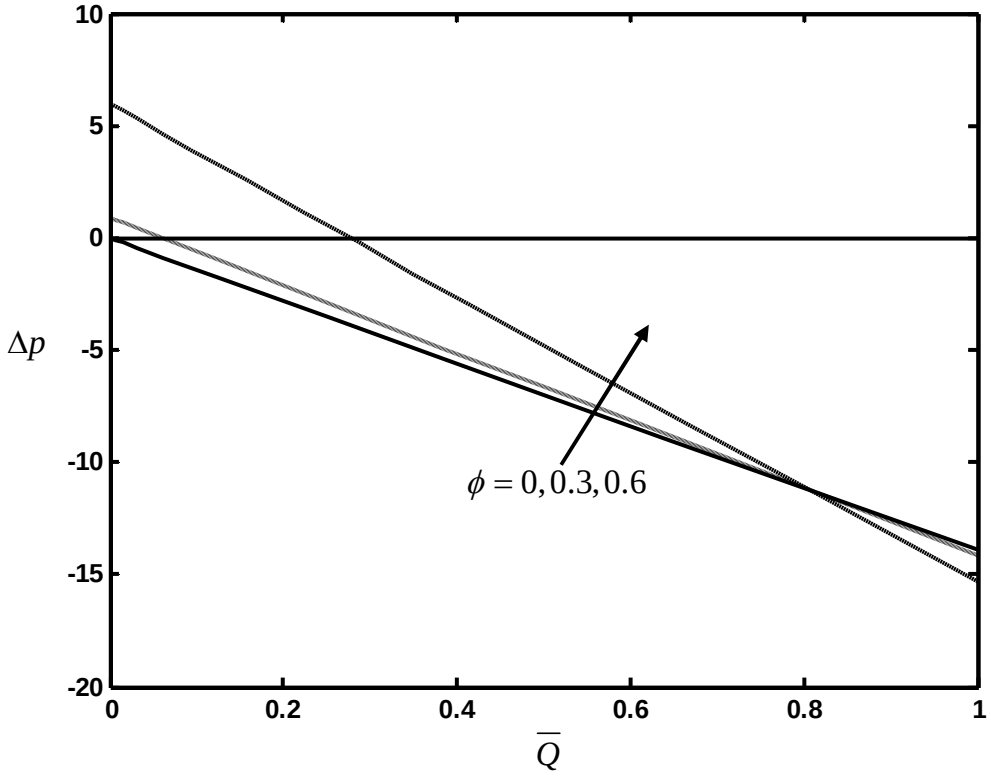

Fig. 5.11 The variation of pressure rise Δp with time-averaged volume flow rate $\overline{Q}$ for different values of ϕ with $\phi = 0.6, We = 0.01,\ n = 0.5$ and $Da = 0.1$.